Plant Growth Regulation (2022) 96:131–144
https://doi.org/10.1007/s10725-021-00765-x

ORIGINAL PAPER

Occurrence of water-soaked brown flesh in Japanese pear (*Pyrus pyrifolia* Nakai) 'Meigetsu' is related to oxidative stress induced by the biological Maillard reaction

Nobuyuki Fukuoka[1] · **Ryusei Watanabe**[1] · **Tatsuro Hamada**[2]

Received: 13 July 2021 / Accepted: 15 October 2021 / Published online: 25 October 2021

Abstract

The occurrence of water-soaked brown flesh in pear fruit is closely related to an activated biological Maillard reaction during the latter half of maturation. In this study, samples of immature and mature pear fruits were assessed for the incidence of water-soaked brown flesh (WSBF), sugar content, expression level of sugar metabolism-related genes, and activity of the Maillard and oxidative stress reactions. The occurrence of WSBF disorder was rare in immature fruit, but was pronounced in mature fruit. Glucose content of the flesh was higher in mature fruit with WSBF than in immature fruit without WSBF. Conversely, sucrose content was inversely correlated to glucose content. Higher levels of the neutral invertase gene *(PpNIV)* were detected in mature fruit compared with immature fruit. Levels of oxidative stress and Maillard reaction products in the flesh of mature fruit were determined. The strongest Maillard and oxidative stress reactions were observed in cells adjacent to the vascular bundle, and these reactions diminished with distance from the vascular bundle. Furthermore, examination of cells near the vascular bundle revealed stronger signal intensity on the phloem side compared to the xylem side. Cellular examination of the phloem side of immature and mature fruits indicated that mature fruit had a stronger signal intensity than immature fruit in both reactions. These results suggest that an increase in the Maillard reaction, attributed to an increased concentration of reducing sugars, during the maturation period may be fundamentally involved in the occurrence of this disorder through oxidative stress.

Keywords Oxidative stress · Flesh cells · Membrane lipid peroxidation · Reducing sugars · Physiological disorder

Abbreviations

ACR	Acrolein
CEL	Nε-(carboxyethyl) lysine
CMA	Nω-(carboxymethyl) arginine
CML	Nε-(carboxymethyl) lysine
CTAB	Cetyltrimethylammonium bromide
DAF	Days after full flowering
3-DG-I	3-Deoxyglucosone-derived hydroimidazolone
DT	Dityrosine
GA	Glycolaldehyde
GA-P	Glycolaldehyde-pyridine
GO	Glyoxal
IgG	Immunoglobulin G
MG	Methylglyoxal
8-NG	8-Nitroguanosine
PpAIV	Acid invertase gene
PpFK	Fructokinase gene
PpHK	Hexokinase gene
PpNAD-SDH	NAD-dependent sorbitol dehydrogenase gene
PpNIV	Neutral invertase gene
PpSPS	Sucrose phosphate synthase gene
PpSUS	Sucrose synthase gene
PBS	Phosphate-buffered saline
ROS	Reactive oxygen species
WSBF	Water-soaked brown flesh

Communicated by Xingfeng Shao.

✉ Nobuyuki Fukuoka
nfukuoka@ishikawa-pu.ac.jp

[1] Experimental Farm, Ishikawa Prefectural University, Nonoichi, Ishikawa, Japan

[2] Research Institute for Bioresources and Biotechnology, Ishikawa Prefectural University, Nonoichi, Ishikawa, Japan

Introduction

Japanese pear (*Pyrus pyrifolia* Nakai) 'Meigetsu' is a red pear cultivar developed by cross-fertilization of Hinoshita/native species around 1780 to 1790. Meigetsu is a late-maturing (mid to late September) cultivar characterized by a fruit weight of around 700 g, which is heavier than normal pears, sugar content of 12% or more, strong tree vigor, and large number of branches (Ishikawa Fruit Tree Gardening Association 1987). However, this cultivar frequently exhibits the physiological disorder known as water-soaked brown flesh (WSBF), in which a region of the fruit's flesh turns brown (Ishikawa Fruit Tree Horticulture Association 1987) (Fig. 1B). This disorder occurs during fruit maturation before harvesting. WSBF makes fruits unmarketable and promotes susceptibility to secondary fungi and bacteria. Therefore, the occurrence of this disorder represents a serious problem for not only farmers but also consumers.

Japanese pear fruits often develop a physiological disorder called watercore, in which a watery translucent region appears in the flesh near the fruit's peel in the latter half of the maturation period. The watercore region turns brown and the flesh cells are often disrupted (Yamaki et al. 1976). The incidence of this disorder increases during late fruit maturation (Kajiura et al. 1976); further, it is promoted by reducing the amount of fruit set to produce large fruits (Sakuma et al. 1995), and decreased by suppressing fruit enlargement by defoliation (Sakuma et al. 1998). WSBF of the pear cultivar Meigetsu is considered to be a physiological disorder similar to watercore, as it is found in the flesh during the latter half of maturation.

Incidentally, there is a physiological disorder of sweet potatoes in which the inside of mature storage roots turns brown (Fukuoka et al. 2018). According to Fukuoka et al. (2020), this disorder is closely related to enhancement of the biological Maillard reaction due to increased concentrations of reducing sugars during maturation; the increase in the Maillard reaction causes intracellular oxidative stress and a consequent accumulation of brown substances. The Maillard reaction produces a brown substance (melanoidins) that is observed when reducing sugars and amino compounds (amino acids, peptides and proteins) are heated. It is known that the Maillard reaction produces reactive oxygen species (ROS) during the reaction process (Lepetsos and Papavassiliou 2016). Increased ROS concentrations in vivo cause peroxidation of membrane lipids, which can cause enzymatic browning (Jambunathan 2010). At the early stage of watercore, higher sorbitol, fructose, and glucose contents were detected in the affected regions compared to healthy regions (Yamaki et al. 1976). Recently, Nishitani et al. (2020) reported that 115 genes, including those related to sugar metabolism, hormones, and the cell wall, were characteristically identified at the region of injury. These facts may suggest that WSBF in Meigetsu is associated with sugar metabolism in the flesh during the latter half of maturation and an accompanying increase in the Maillard reaction. However, studies of the Maillard reaction in growing plants have only recently been conducted on the leaves of *Arabidopsis* (Paudel et al. 2016) and the root nodules of legume family plants (Manuel et al. 2018). Moreover, research on storage organs has also been limited to the storage roots of sweet potato (Fukuoka et al. 2020) and radish (Fukuoka et al. 2021). To our knowledge, there have been no studies of the Maillard reaction in tree-borne fruits.

The aim of this study is to clarify whether the cause of WSBF in the flesh near the pericarp in the latter half of the maturation period is related to enhancement of the biological Maillard reaction due to sugar metabolism. Therefore, immature and mature fruits at different fruit maturation stages were collected, and an expression analysis of sugar metabolism-related genes and an immunohistochemical analysis of metabolites involved in the Maillard reaction were performed. In this paper, we propose that increases in the Maillard reaction due to elevated concentrations of reducing sugars during the maturation period may be fundamentally involved in the occurrence of this disorder.

Materials and methods

Plant materials and sampling methods

The material used in this study was Japanese pear (*Pyrus pyrifolia* Nakai) cultivar Meigetsu (15th grade, top grafting to cultivar Shinsui in 2005) planted on the farm associated with Ishikawa Prefectural University. The budding and leaf-spreading periods began on March 12 and March 31, 2020, respectively. The flowering start period, flowering peak period, and flowering end period were April 10, April 12, and April 23, 2020, respectively. A basal fertilizer of 7.8 g m^{-2} N, 6.9 g m^{-2} P_2O_5, and 6.9 g m^{-2} K_2O, dolomite (Kumiai magnesium lime, Ueda Lime Manufacturing Co., Ltd., Gifu, Japan) at 44 g m^{-2}, fused magnesium phosphate (Hinode Sangyo Co., Ltd., Kanagawa, Japan) at 44 g m^{-2}, and 4.4 g m^{-2} micro-elemental manure (Toujitsu Kasei Co., Ltd., Hyogo, Japan) containing 0.4 g/100 g Mn, 0.3 g/100 g B, 1.2 g/100 g Fe, and 0.03 g/100 g Cu were applied on December 19, 2019. As a top dressing, 3.8 and 4.3 g m^{-2} N, 2.7 and 2.7 g m^{-2} P_2O_5, and 3.2 and 3.8 g m^{-2} K_2O were applied on April 14 and June 5, 2020, respectively.

On September 28, about 170 days after full flowering (DAF), 25 immature fruit with ground color 1–2 and mature fruit with ground color 3–4 were collected per group. Next,

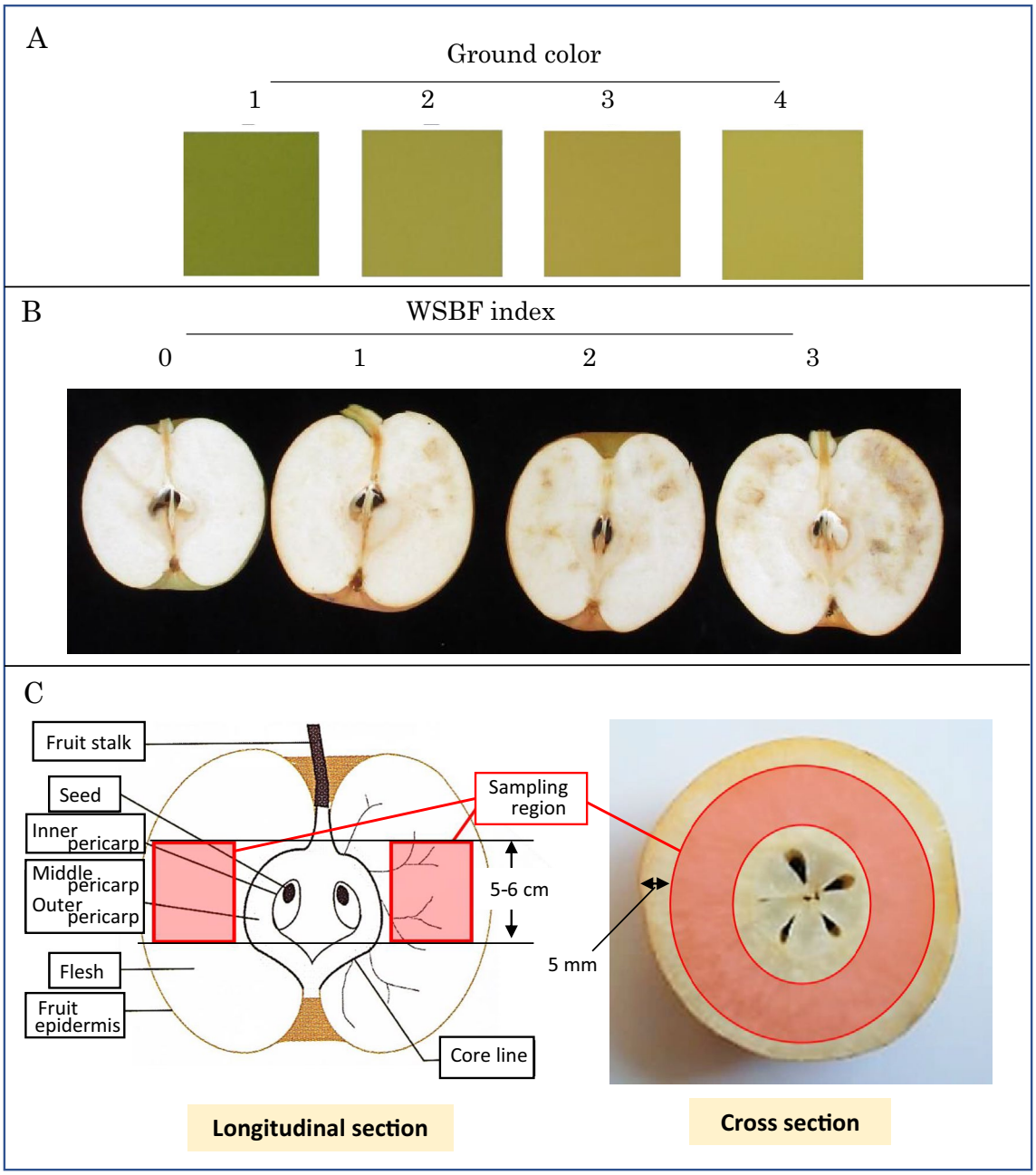

Fig. 1 The ground color (**A**), severity of WSBF disorder (**B**), and sampling region for analysis of sugar content and sugar-related gene expression (**C**) of pear fruit in this study. The ground color of fruit was measured in reference to the fruit color chart of Japanese pear (ground color) (National Institute of Fruit Tree Science, Ministry of Agriculture, Japan). The fruit was cut lengthwise along the central axis and the severity of WSBF was scored by visual inspection based on four levels of discoloration: none (WSBF index, 0), slight (WSBF index, 1), moderate (WSBF index, 2), or severe (WSBF index, 3). For analysis of sugar content and sugar-related gene expression, a cylindrical disk with a thickness of about 5–6 cm was collected from the midportion of fruit using a table knife. After removing both the 5-mm-thick flesh on the epidermis and the pericarp located in the center, the remaining flesh was shredded with a table knife, frozen in liquid nitrogen and stored at − 45 °C

16–18 medium-sized fruit per group were selected and used to measure fruit growth and the occurrence of WSBF. The ground color of fruit was measured in reference to the fruit color chart of Japanese pear (ground color) (National Institute of Fruit Tree Science, Ministry of Agriculture, Japan) (Fig. 1A). The immature fruit was composed of 50% of ground color 1 fruit and 50% of ground color 2 fruit, and the mature fruit was composed of 50% of ground color 3 fruit and 50% of ground color 4 fruit. To evaluate WSBF disorder, the fruit were cut lengthwise along the central axis

and the severity of WSBF was classified by visual inspection based on four levels of discoloration: None (WSBF index, 0), slight (WSBF index, 1), moderate (WSBF index, 2), or severe (WSBF index, 3) (Fig. 1B). The incidence and severity of WSBF disorder were respectively calculated as follows: *Incidence of WSBF disorder* = *(number of fruit exhibiting WSBF disorder)* × 100/*(number of fruit evaluated)*, and *Severity of WSBF disorder* = Σ *(value of WSBF index in each fruit)* × 100/*(number of fruit investigated* × 4).

Sugar content and the expression of related genes were examined in immature fruit with WSBF index 0 and in mature fruit with WSBF index 1 and 2, since these best represent the symptoms of WSBF at each maturation stage. A cylindrical disk with a thickness of about 5–6 cm was collected from the midportion of the fruit using a table knife. After removing both the 5 mm thick flesh on the epidermis and the pericarp located in the center, the remaining flesh was minced with a table knife, frozen in liquid nitrogen and stored at − 45 °C (Fig. 1C). Analyses were performed on 4–5 biological replicates. For immunohistochemical observation, a tissue mass approximately 1.5 cm on a side per side was excised from the same region used for the sugar analysis. The tissue was fixed with 4% paraformaldehyde in phosphate buffer for 2–3 days at room temperature. The fixed tissue was subsequently dehydrated with an ethanol series (30, 50, 70, 90, 95, and 100%) prior to embedding in a paraffin block. The paraffin block was cut into 10-µm thick slices using a sliding microtome (Daiwa Koki, Saitama, Japan). Sections were placed on silane-coated glass slides, incubated overnight on a hot plate at 50 °C, and then stored at 4 °C.

Sugar content

To measure the sugar content, 20 mL of 80% ethanol was added to 1.0 g of the frozen sample and homogenized. Sugars were extracted with boiling water at 80 °C for 1 h, the sample was centrifuged at 10,000 rpm for 10 min and the supernatant was collected. The sediment was extracted twice using the same method. The supernatants were combined, brought up to 100 ml, and then diluted 20-fold with distilled water. The diluted solution was filtered through a 0.45-µm membrane filter (DISMIC-25CS; Toyo Roshi, Tokyo, Japan). A 10-µl aliquot of this solution was injected into a Dionex ICS-3000 system with a CarboPac PA-1 column (4 × 250 mm) (Dionex, Sunnyvale, CA, USA) for high-performance anion-exchange chromatography with pulsed amperometric detection with 0.25 ml·min^{-1} eluent flow at 30 °C. For analysis, a linear gradient elution program was applied, and elution was carried out with eluent A (125 mmol sodium hydroxide (NaOH)) and eluent B (250 mmol Na-acetate/1 mol NaOH) as the mobile phase at a flow rate of 1 ml·min^{-1}. Sorbitol, glucose, fructose, and sucrose standards were purchased from Nacalai Tesque, Inc. (Kyoto, Japan).

Expression analysis of sugar metabolism genes

Total RNA was purified by a modified cetyltrimethylammonium bromide (CTAB) method (Kim and Hamada 2005). First-strand cDNA was synthesized from the total RNA using ReverTra Ace® qPCR RT Master Mix with gDNA Remover (Toyobo, Osaka, Japan). Real-time PCR was performed on the StepOnePlus™ RT PCR System (Life Technologies, MA, USA) using KOD SYBR® qPCR Mix (Toyobo). The following seven sugar metabolism-related genes were used: NAD-dependent sorbitol dehydrogenase gene (*PpNAD-SDH*; GenBank accession No. KC506731), neutral invertase gene (*PpNIV*; Wang et al. 2020), sucrose phosphate synthase gene (*PpSPS*; GenBank accession No. AB334114), hexokinase gene (*PpHK*; Wang et al. 2020), fructokinase gene (*PpFK*, Wang et al. 2020), acid invertase gene (*PpAIV*; GenBank accession No. AB334115), and sucrose synthase gene (*PpSUS*; Itai et al. 2015). Nucleotide sequences of the primers are shown in Supplementary Table S1. Relative gene expression was quantified using the ΔΔCT method.

Immunohistochemical observation

Oxidative stress evaluation was performed using anti-8-nitroguanosine (8-NG) monoclonal antibody, anti-dityrosine (DT) monoclonal antibody, and anti-acrolein (ACR) monoclonal antibody purchased from JaICA (Japan Institute for Aging and Control, Shizuoka, Japan). To evaluate the Maillard reaction, anti-methylglyoxal (MG) monoclonal antibody, anti-3-deoxyglucosone-derived hydroimidazolone (3-DG-I) monoclonal antibody, anti-Nε-(carboxymethyl) lysine (CML) monoclonal antibody, and anti-glycolaldehyde-pyridine (GA-P) monoclonal antibody were used (Trans Genic Inc., Kobe, Japan). These antibodies were all mouse-derived immunoglobulin G (IgG) antibodies. The characteristics of each monoclonal antibody are shown in Supplementary Table S2. Except for GA-P, the primary antibodies were diluted 1:100 with phosphate-buffered saline (PBS) (containing 1 g/100 ml bovine serum albumin (BSA). GA-P was diluted 1:200 with PBS. Sodium azide (NaN_3) (0.1 g/100 ml) was added for dilution of the ACR and MG antibodies only.

Procedures for deparaffinization, optimal antigen retrieval, inactivation of endogenous peroxidase, and primary antibody treatment were performed according to our previous report (Fukuoka et al. 2020). Secondary antibody treatment was performed using the Histofine Mouse Stain Kit (Nichirei Bioscience, Tokyo, Japan), and the staining procedure was performed according to the manufacturer's

instructions. Immune complexes were visualized using a liquid DAB substrate chromogen system (Agilent Technologies, CA, USA). Negative controls consisted of tissue sections from each specimen, processed in parallel with omission of the primary antibody. Tissue sections were dehydrated with ethanol and xylene, and finally mounted in mounting medium (Mount-Quick; Daido Sangyo, Tokyo, Japan). The sections were imaged at 400 × magnification under light microscope (MT5300 L; Meiji Techno, Saitama, Japan) and images were digitized using EOS Utility software (Canon, Tokyo, Japan). For immunohistochemical signal quantification, the brown region was measured using NIH Image software (http://www.rsb/info.nih.gov/nih-image) as described previously (Fukuoka et al. 2020).

Statistical analysis

Statistical analysis was performed using the software package Ekuseru-Toukei Ver. 7 (Social Survey Research Information Co., Ltd., Tokyo, Japan). Comparison of means was performed with Tukey–Kramer's or Duncan's multiple range test at $P < 0.05$.

Results

Incidence of WSBF disorder

The presented data in Table 1 shows the effect of maturation stage (ground color) on the occurrence of WSBF disorder. In immature fruit with ground colors 1 and 2, the incidence of fruit with WSBF index 0 and 1 was 89 and 11%, respectively, and no fruit graded as WSBF index 2 or higher was observed. In contrast, in mature fruit with ground colors 3 to 4, the severity of WSBF progressed significantly, and the incidence of fruit with WSBF index 0, 1, 2, and 3 reached 19, 31, 31, and 19%, respectively. As a result, the calculated value of severity in immature fruit was only 3.7, while that in mature fruit reached approximately 50.

Table 1 Effect of fruit maturation stage on the occurrence and severity of WSBF in pear fruits

Maturation stage	Fruits with WSBF (%)				Severity of WSBF
	0	1	2	3	
Immature	89	11	0	0	3.7
Mature	18.8	31.3	31.3	18.8	50

The fruit was cut lengthwise along the central axis and the severity of WSBF was scored by visual inspection based on four levels of discoloration: None (WSBF index, 0), slight (WSBF index, 1), moderate (WSBF index, 2), or severe (WSBF index, 3). The incidence and severity of WSBF disorder were respectively calculated as follows: IncidenceofWSBFdisorder = (numberoffruitsexhibitingWSBFdisorder) × 100/(numberoffruitsinvestigated), and SeverityofWSBFdisorder = Σ(valueofWSBFindexineachfruit) × 100/(numberoffruits investigated × 4)

WSBF water-soaked brown flesh

Comparison of sugar content between immature and mature fruits

No clear correlation was found between the content of sorbitol or fructose and the degree of fruit maturity (Fig. 2A, C). In contrast, as fruit maturation progressed, glucose content increased and sucrose content concomitantly decreased (Fig. 2B, D). This tendency was more pronounced in fruit with WSBF index 2 than in fruit with WSBF index 1. The glucose content in fruit with WSBF index 2 was about 190% of that in fruit with WSBF index 1, while the sucrose content in the former was only about 32% of that in the latter.

Comparison of sugar-related gene expression between immature and mature fruits

The expression level of *PpNIV* increased as fruit maturation progressed, and this trend was more pronounced in fruit with WSBF index 2 than in fruit with WSBF index 1 (Fig. 3C). The level in mature fruit with WSBF index 1 and 2 was about 1.8 and 2.8 times higher than that in immature fruit with WSBF index 0, respectively. The expression levels of *PpAIV* and *PpFK1* in mature fruit with WSBF index 1 were similar to those in immature fruit with WSBF index 0; however, higher levels were detected in mature fruit with WSBF index 2 (Fig. 3B, J). On the other hand, *PpNAD-SDH* expression level tended to decrease as the fruit matured, although no statistically significant difference between immature fruit with WSBF index 0 and mature fruit with WSBF index 1 was observed (Fig. 3A). There was no statistically significant difference in the expression of *PpSUS* and *PpHK* between immature and mature fruits (Fig. 3D, F).

Accumulation of Maillard reaction (CML) and oxidative stress (ACR) products in pear flesh with WSBF disorder

Using the sections obtained from mature fruit with WSBF index 2, the characteristics of accumulated oxidative stress and Maillard reaction products in the flesh were determined. Signal intensity of the Maillard reaction product (CML) was strong in the vascular bundle (Fig. 4A, E) and stone cells (Fig. 4C, G), as well as in flesh cells adjacent to these organs (Fig. 4I, K). However, in flesh cells, the staining intensity weakened with increasing distance from these organs (Fig. 4M, O, Q, S). Similarly, the signal intensity of oxidative stress product (ACR) was stronger in the vascular

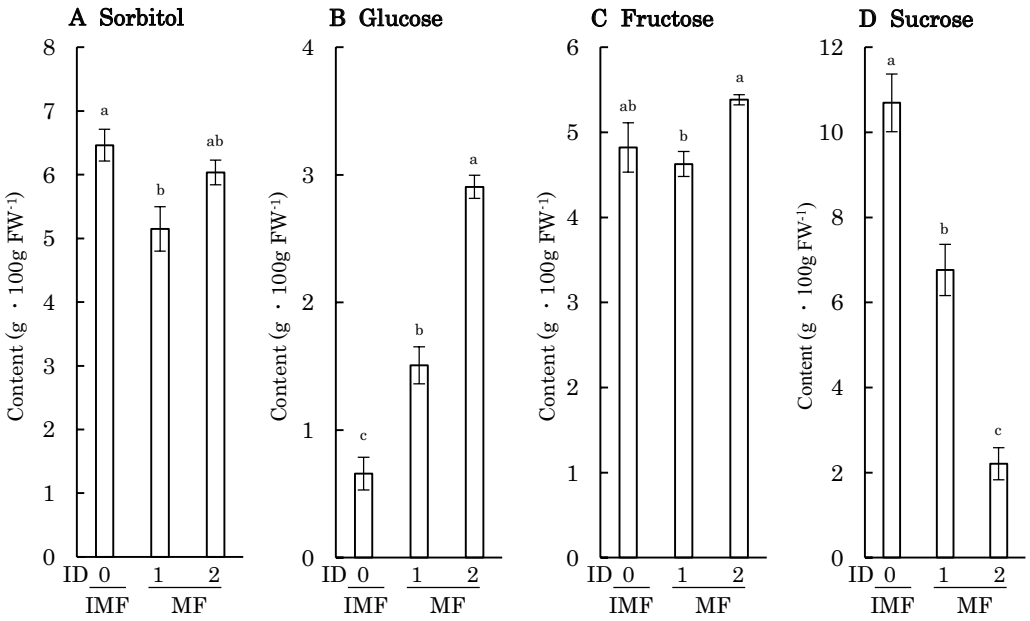

Fig. 2 Relationship between the severity of WSBF disorder and contents of sorbitol (**A**), glucose (**B**), fructose (**C**), and sucrose (**D**) in pear fruit. Sugar content was examined using samples with WSBF index 0 from immature fruit and WSBF index 1 and 2 from mature fruit. Error bars indicate ± SE (n = 5). Different letters indicate significant differences at the 5% level by Tukey's multiple range test

bundle (Fig. 4F), stone cells (Fig. 4H), and flesh cells adjacent to these organs (Fig. 4J, L), and the intensity weakened as the distance from these organs increased (Fig. 4N, P, R, T).

In flesh cells around the vascular bundle, the characteristics of accumulated Maillard reaction and oxidative stress products were different between the xylem side and the phloem side. Signal intensity of the Maillard reaction product (CML) was stronger in flesh cells on the phloem side (Fig. 5B, E) than on the xylem side (Fig. 5B, H). Likewise, stronger signal intensity of the oxidative stress product (ACR) was observed in flesh cells on the phloem side (Fig. 5C, F) compared to the xylem side (Fig. 5C, I).

Comparison of accumulation of oxidative stress products (8-NG, DT, ACR) between immature and mature fruits

The correlation between the degree of fruit maturity and the accumulation of oxidative stress products was compared in phloem-side flesh cells using immature fruit with WSBF index 0 and mature fruit with WSBF index 1 and 2. Although the signal intensity of 8-NG, DT, and ACR increased as fruit maturation progressed, this trend was more pronounced with DT and ACR than with 8-NG (Fig. 6A–I); a stronger signal was detected in flesh cells of mature fruit with WSBF index 1 compared to those of immature fruit with WSBF index 0, and this trend was enhanced in mature fruit with WSBF index 2. The calculated staining intensities for these antibodies, obtained by image analysis, are shown in Fig. 6J. The values for 8-NG, DT, and ACR in flesh cells of mature fruit with WSBF index 1 were 2.6, 3.0, and 2.0 times greater than those in immature fruit with WSBF index 0, respectively. The values in flesh cells of mature fruit with WSBF index 2 were 2.4, 4.0, and 3.4 times greater than those in immature fruit with WSBF index 0, respectively.

Comparison of accumulation of Maillard reaction products between immature and mature fruits

The Maillard reaction products were evaluated using MG, 3-DG-I, CML, and GA-P. As with oxidative stress, signal intensities of all Maillard reaction biomarkers increased in flesh cells of mature fruit compared to those of immature fruit; however, mature fruit with WSBF index 1 and 2 showed similar signal intensities (Fig. 7A–L). Results of calculated staining intensities are shown in Fig. 7M. The values for MG, 3-DG-I, CML, and GA-P in flesh cells of mature fruit with WSBF index 1 were 3.7, 2.4, 2.9, and 2.1 times greater than those in immature fruit with WSBF index 0, respectively. In addition, these values in mature fruit with WSBF index 1 and 2 were not significantly different.

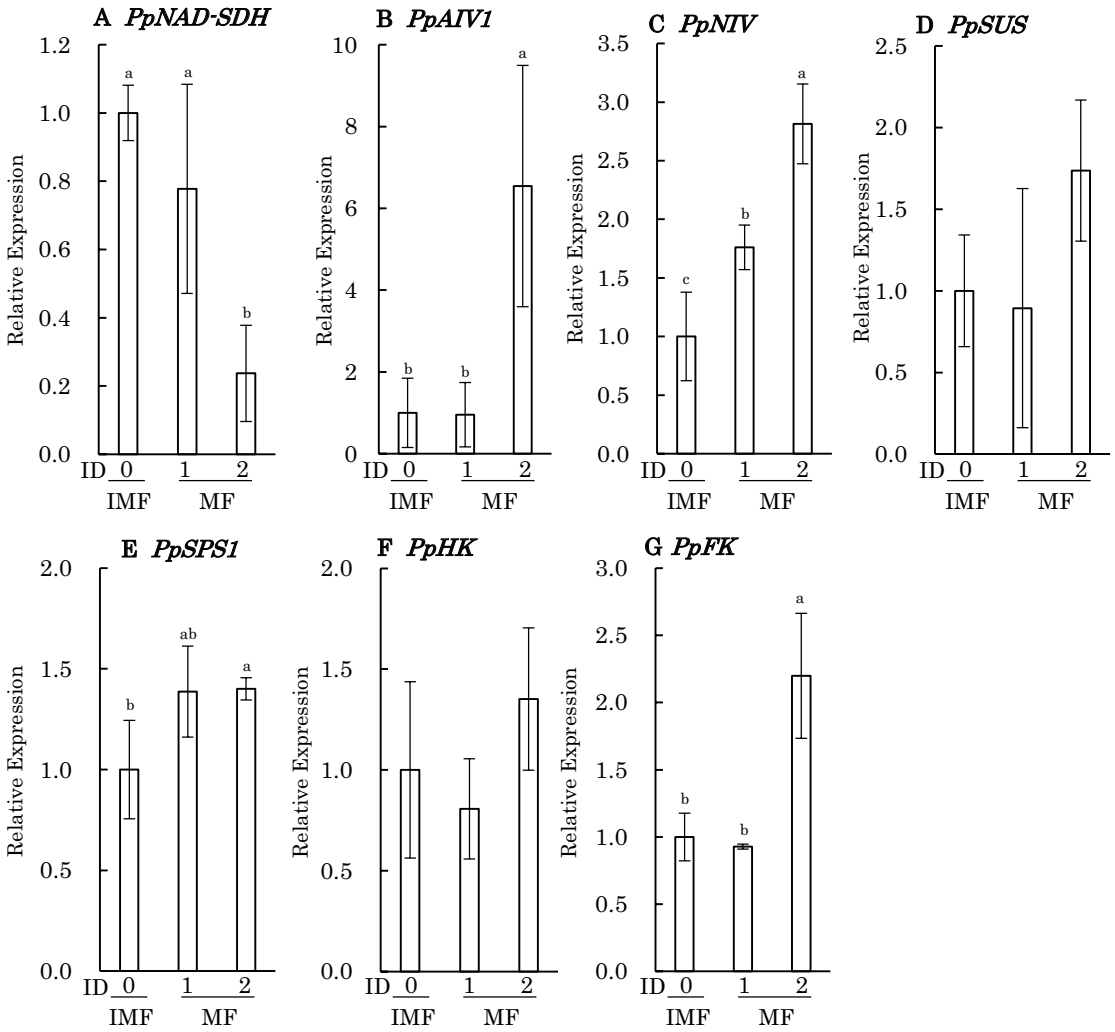

Fig. 3 Relationship between the severity of WSBF disorder and sugar metabolism-related gene expression in pear fruit. **A**, **B**, **C**, **D**, **E**, **F**, and **G** indicate NAD-dependent sorbitol dehydrogenase gene (PpNAD-SDH), acid invertase gene (PpAIV;), neutral invertase gene (PpNIV), sucrose synthase gene (PpSUS), sucrose phosphate synthase gene (PpSPS), hexokinase gene (PpHK), and fructokinase gene (PpFK), respectively. Gene expression was examined using the samples with WSBF index 0 from immature fruit and WSBF index 1 and 2 from mature fruit. Error bars indicate ± SE (n = 3-5). Different letters indicate significant differences at the 5% level by Duncan's multiple range test

Discussion

The Maillard reaction is initiated by a condensation reaction involving reducing sugars and amino acids (Ames 1992). This reaction produces various carbonyl compounds from Schiff bases and Amadori compounds, which react with amino acids to produce various advanced glycation end products (AGEs) (Murata 2019). Carbonyl compounds produced during the Maillard reaction include glyoxal (GO), glycolaldehyde (GA), MG, 3-deoxyglucosone (3-DG), etc., each of which reacts with amino acids and produces unique AGEs. For example, GO causes the formation of Nε-(carboxymethyl) lysine (CML) (Al-Abed and Bucala 1995). Additional AGEs formed by GO include glyoxal-derived lysine dimer (Wells-Knecht et al. 1995) and Nω-(carboxymethyl) arginine (CMA) (Glomb and Lang 2001). GA promotes CML formation (Anderson 2003), and MG causes the generation of, for example, Nε-(carboxyethyl) lysine (CEL) (Ahmed et al. 1997). 3-DG leads to the formation of pyrraline (Portero-Otin et al. 1995) and 3-DG-I (Singh et al. 2001). In this study, WSBF disorder progressed significantly in mature fruit compared to immature fruit (Table 1). Correspondingly, the accumulation of Maillard reaction products, such as MG, CML, GA-P, and 3-DG-I, was greater in flesh cells of mature fruit than in those of immature fruit (Fig. 7). It has been reported that the Maillard reaction is enhanced when *Arabidopsis* leaves are subjected to drought stress, in which case CML production

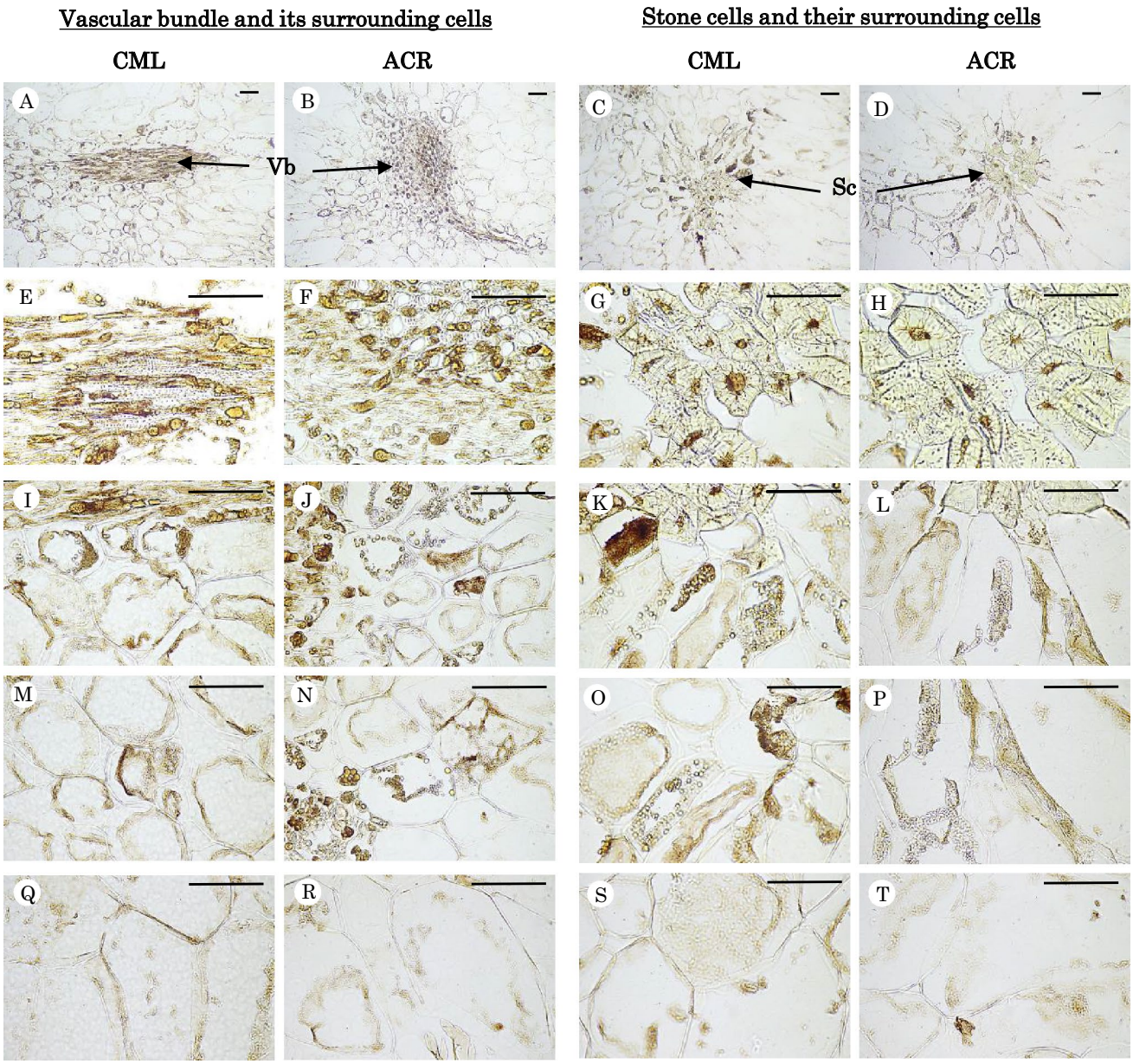

Fig. 4 Comparison of the accumulation of Maillard reaction product, CML (**A**, **C**, **E**, **G**, **I**, **K**, **M**, **O**, **Q**, **S**) and oxidative stress product, ACR (**B**, **D**, **F**, **H**, **J**, **L**, **N**, **P**, **R**, **T**) in regions around vascular bundles and stone cells. Left photos indicate the vascular bundle (**A**, **B**, **E**, F) and its surrounding cells (**A**, **B**, **I**, **J**, **M**, **N**, **Q**, **R**). Right photos indicate stone cells (**C**, **D**, **G**, **H**) and their surrounding cells (**C**, **D**, **K**, **L**, **O**, **P**, **S**, **T**). **I**, **J** flesh cells adjacent to the vascular bundle, **M**, **N** flesh cells near the vascular bundle, **Q**, **R** flesh cells away from the vascular bundle, **K**, **L** flesh cells adjacent to the stone cells, **O**, **P** flesh cells near the stone cells, **S**, **T** flesh cells away from the stone cells. *Vs* vascular bundle, *Sc* stone cells. Each scale bar shows 100 mm

mainly via GO occurs (Paudel et al. 2016). In sweet potatoes, a physiological disorder occurs in which the inside of the storage root turns brown in the latter half of the maturation period (Fukuoka et al. 2020). In this case, Maillard reaction products, such as MG and 3-DG-I, are remarkably accumulated as the disorder progresses. Likewise, in Japanese radish, it has been reported that internal browning occurs in the latter half of growth, and there is a strong correlation between the accumulation of AGEs and the severity of the disorder (Fukuoka and Hamada 2021). As mentioned above, in this study, the progression of WSBF disorder resulted in increased accumulation of a wide range of Maillard reaction products, such as GA-P and 3-DG-I, in addition to MG and CML. These results suggest that the development of WSBF disorder observed in mature-stage pear fruit may be largely dependent on the activation of a wide range of Maillard

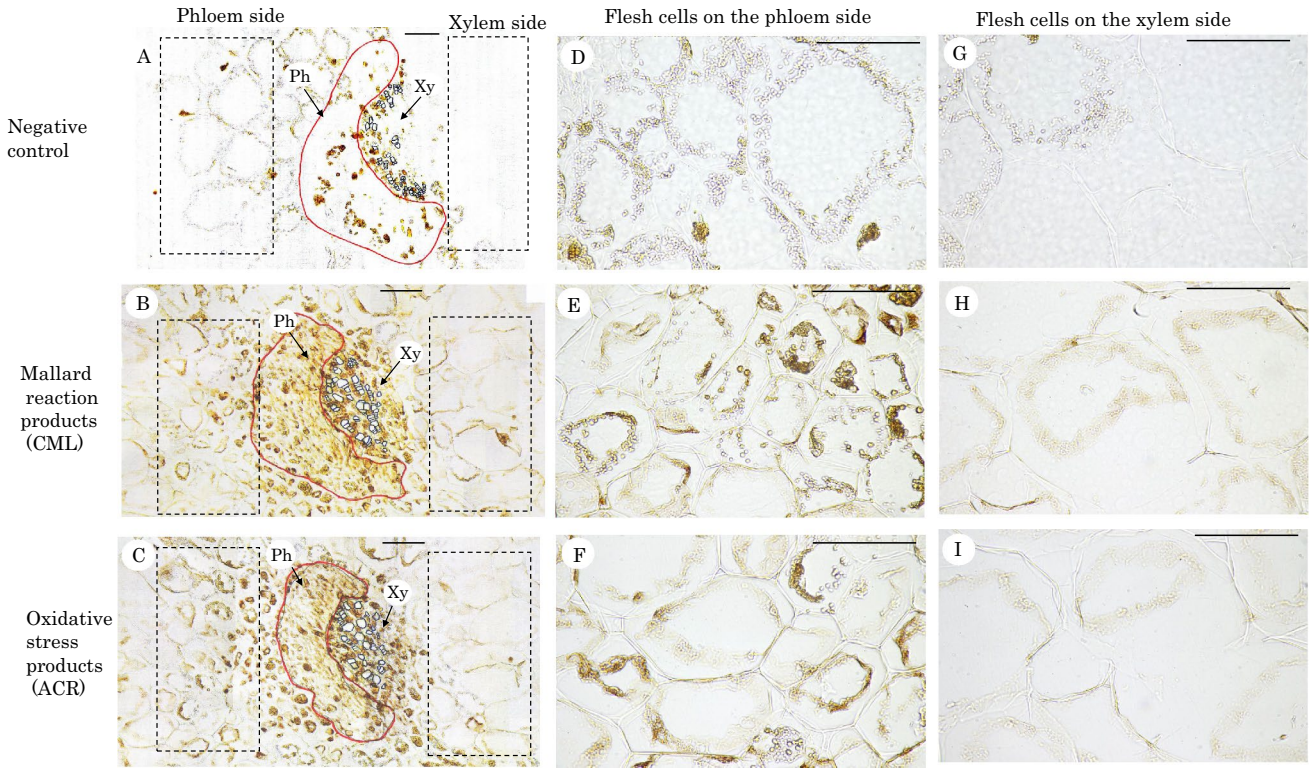

Fig. 5 Comparison of the accumulation characteristics of Maillard reaction products (**B**, **E**, **H**) and oxidative stress products (**C**, **F**, **I**) in flesh cells around the vascular bundle. Ph surrounded by the red line and Xy in **A**, **B**, and **C** indicate the phloem and xylem regions, respectively. The regions surrounded by the black dashed line on the left side in **A**, **B**, and **C** show the flesh cells on the phloem side. **D**, **E**, and **F** are enlargements of the left regions in **A**, **B** and **C**, respectively. The regions surrounded by the black dashed line on the right side in **A**, **B**, and **C** show the flesh cells on the xylem side. **G**, **H** and **I** are enlargements of the right regions in **A**, **B** and **C**, respectively. **A**, **D** and **G** indicate negative control. Each scale bar shows 100 mm

reaction pathways. Substances produced in the early stage of the Maillard reaction include those with physicochemical properties such as browning, fluorescence, and crosslink formation (Murata 2019). In the latter stage of the Maillard reaction, substances called melanoidins (brown-colored) are produced. Thus, the browning phenomenon shown in the flesh of pear fruit may be due to the accumulation of browning substances caused by the Maillard reaction.

In mammals (human) and arthropods (silkworm), the biological Maillard reaction is enhanced when blood sugar concentrations increase (Singh et al. 2001; Matsumoto et al. 2011). It has been reported that the Maillard reaction is promoted and the concentration of reducing sugars increases in regions where internal browning of sweet potato tubers appears (Fukuoka et al. 2020). Since the Maillard reaction was enhanced in pear fruit with the progression of WSBF, it is possible that excessive sugar accumulation occurred in the damaged regions. In this study, quantitative analysis of the main sugars of pear fruit (sorbitol, glucose, fructose, and sucrose) was performed. Furthermore, expression analysis of genes related to sugar metabolism was conducted. Results revealed that the glucose content increased and the sucrose content decreased in fruit as fruit maturation progressed (Fig. 2). In addition, in mature fruit, this trend was remarkable in fruit with more profound WSBF disorder. On the other hand, there was no difference in fructose content between mature and immature fruits. The results of gene expression analysis showed that *PpNAD-SDH* levels decreased in mature fruit compared to immature fruit (Fig. 3). Conversely, *PpNIV* levels increased with increasing fruit maturity. *PpAIV* and *PpFK* expression levels did not differ between mature fruit with mild WSBF and immature healthy fruit; however, levels were increased in mature fruits with more severe WSBF.

In Japanese pears, the sugar alcohol sorbitol is known to be a translocation sugar (Zhang et al. 2014). Sorbitol translocated from the leaves to the fruit is converted to fructose and glucose by catalysis of NAD-SDH and sorbitol oxidase (SOX), respectively (Bianco and Rieger 2002; Teo et al. 2006). Next, fructose is catalyzed by fructokinase and glucose is catalyzed by hexokinase to produce intermediate metabolites, and the produced intermediate metabolites are catalyzed by sucrose phosphate synthase to generate sucrose (Tanase and Yamaki 2000; Yamaki and Moriguchi 1989).

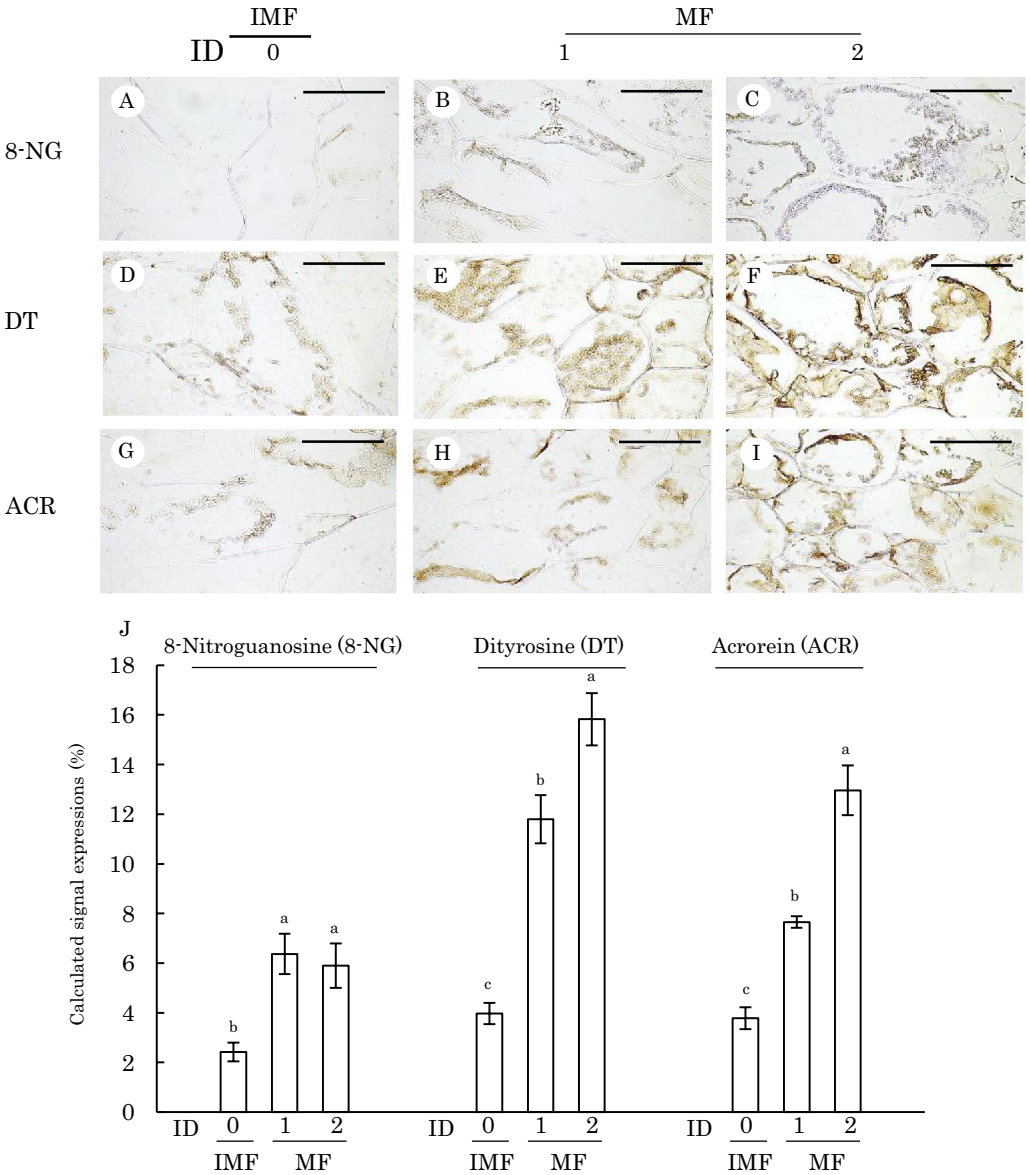

Fig. 6 Immunohistochemical staining (**A–I**) and signal intensities (**J**) of the oxidative stress in flesh cells with WSBF index (ID) 0 from immature fruit (IMF) and WSBF ID 1 and 2 from mature fruit (MF). **A–C** 8-NG, **D–F** DT, **G–I** ACR. The photos show the flesh cells on the phloem side of the vascular bundle.. Each scale bar shows 100 µm. Values in the graph are presented as the mean ± SE (n = 8). Different lowercase letters above the bars indicate significant differences at the 5% level by Tukey's range test

Furthermore, sucrose is broken down into fructose and glucose by invertase (IV) (Hashizume et al. 2003). In this study, the decrease in sucrose content and increase in glucose content with the progression of fruit maturity is suggested to be attributable to increased *NIV* gene expression (Fig. 3). However, there was no apparent correlation between fruit fructose content and the degree of fruit maturity. The reason why there was no difference in fructose content in the early stages of WSBF development may be attributed to lower fructose supply as a result of decreased *NAD-SDH* gene expression and higher fructose production due to increased *NIV* gene expression. In addition to the above, the reason why there was no difference in fructose content with more advanced WSBF may be related to higher fructose consumption due to increased *FK* gene expression and higher fructose production due to increased *AIV* gene expression. As shown above, the Maillard reaction starts with a reaction between reducing sugars and amino acids. Hence, we consider that the increase in glucose concentrations due to higher neutral invertase activity enhances the biological Maillard reaction, and the resulting metabolic change triggers the occurrence of WSBF disorder. Yamaki et al. (1976) reported that at an

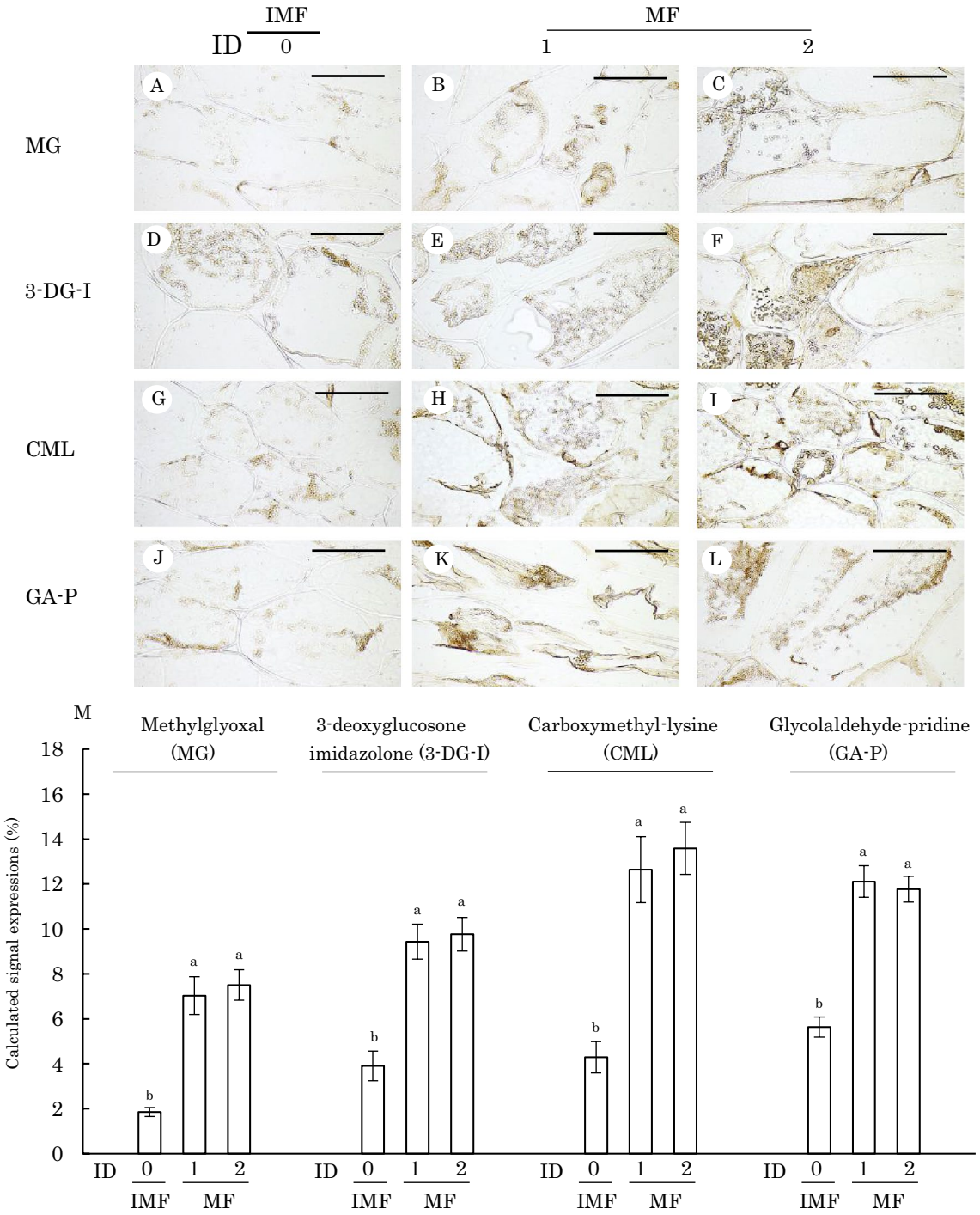

Fig. 7 Immunohistochemical staining (**A**–**L**) and signal intensities (**M**) of the Maillard reaction products in flesh cells with WSBF index (ID) 0 from immature fruit (IMF) and WSBF ID 1 and 2 from mature fruit (MF). **A**–**C** MG, **D**–**F** 3-DG-I, **G**–**I** CML, **J**–**L** GA-P. The photos show the flesh cells on the phloem side of the vascular bundle. Each scale bar shows 100 μm. Values in the graph are presented as the mean ± SE (n = 8). Different lowercase letters above the bars indicate significant differences at the 5% level by Tukey's range test

early stage of watercore, higher contents of sorbitol, fructose, and glucose were detected in affected regions compared to healthy regions. Furthermore, regarding intervarietal differences of watercore disorder, higher *IV* gene expression was detected in susceptible sibs than in resistant sibs (Nishitani et al. 2020).

Sorbitol that has moved to the fruit passes through the phloem of the vascular bundle; it is translocated via the

apoplasm into flesh cells (Zhang et al. 2014), converted to glucose, fructose, and sucrose, and then transported to the surrounding flesh cells via a sugar transporter (Yamaki 2007). These facts suggest that sugar concentrations in flesh tissue are higher in the phloem side than in the xylem side, and that flesh cells near the vascular tissue have higher sugar concentrations than cells distal to the vascular bundle. This study also examined the organ specificity of the accumulation of Maillard reaction products in the flesh region. Our results showed that the accumulation of Maillard reaction products was particularly prominent in vascular bundles and stone cells, as well as in flesh cells adjacent to these organs; consequently, the amount of Maillard reaction products accumulated in flesh cells decreased as the distance from these organs increased (Fig. 4). Furthermore, the observed accumulation of Maillard reaction products in flesh cells around the vascular bundles indicated that the accumulation is clearly enhanced in phloem-side flesh cells compared with xylem-side cells (Fig. 5). Therefore, significant increases in the accumulation of Maillard reaction products in phloem-side flesh cells is probably due to increases in sugar concentrations in this region, resulting from the pattern of sugar transport in fruit. In this study, the accumulation of Maillard reaction products was remarkable, even in flesh cells around stone cells. However, the role of stone cells in pear fruit is currently unknown; thus, further investigation is needed to determine why the Maillard reaction was activated around stone cells.

In this study, 8-NG and DT were used as biomarkers of oxidative damage in DNA and proteins, respectively (Akuta et al. 2006; DiMarco and Giulivi 2007), and ACR was used as a biomarker of lipid peroxidation to assess the oxidative stress response (Uchida 1999). An important finding in this study was that the accumulation of Maillard and oxidative stress reaction products was observed in almost the same region. The extent of ACR accumulation increased especially in the flesh region adjacent to the vascular bundle where the disorder progressed and the Maillard reaction was enhanced (Fig. 4). Similarly, accumulation of oxidative stress products was increased in phloem-side flesh cells, which showed a large elevation in the Maillard reaction (Fig. 5). An additional important finding was that in mature fruits, differences in the accumulation of oxidative stress and Maillard reaction products were observed depending on the progression of WSBF disorder (Figs. 6, 7). That is, in mature fruit, a high accumulation of Maillard reaction products was consistently observed regardless of the degree of WSBF, while lower levels of oxidative stress products accumulated in mildly damaged fruit compared to severely damaged fruit. In animal cells, AGEs produced by the Maillard reaction are known to send an inflammatory signal by interacting with a receptor embedded in the cell membrane, and the ROS concentration increases through activation of NADPH oxidase (Tarafdar and Pula 2018). Teshima et al. (2014) reported that high intracellular glucose concentrations oxidize glucose-derived pyruvate and increase the influx of electron transport chain donors into the mitochondrial respiratory chain. As a result, hyperpolarization of the inner mitochondrial membrane potential occurs, electron transfer in complex III is partially inhibited, and electrons are accumulated in ubisemiquinone to produce superoxide (Nishikawa et al. 2000). From these facts, it is possible that increases in intracellular monosaccharide concentration and the Maillard reaction induce overproduction of ROS, resulting in an oxidative stress reaction. We considered that activation of the Maillard reaction by increasing sugar concentration induces the production of ROS, and as a result, various oxidative stress reactions occur.

Generally, polyphenol oxidase (PPO) is localized in the amyloplast of cells, and polyphenols are present in vacuoles, and the two do not react (Murata and Homma 1998). When membrane collapse occurs due to lipid peroxidation, PPO and polyphenols are released into the cytosol from each organelle, and an enzymatic browning reaction occurs between the two. Since lipid peroxidation due to oxidative stress occurred in WSBF damaged flesh cells as described above, another possible cause of the browning phenomenon in the flesh of pear fruit is thought to be excessive ROS production, followed by an enzymatic reaction due to membrane collapse. In sweet potato, the inside of storage roots turns brown during the maturation period; however, in this case, it has been reported that in addition to the enhancement of the Maillard reaction, peroxidation of membrane lipids occurs due to oxidative stress, and polyphenol compounds accumulate (Fukuoka et al. 2020).

Conclusions

This study examined the etiology of WSBF disorder in pear fruit immunohistologically and presented a new scheme that has not previously been considered for its causes. That is, the increase in reducing sugar concentration in the latter half of ripening in the fruit triggers the Maillard reaction, which results in oxidative stress. This increase in oxidative stress also causes peroxidation of membrane lipids. The browning substances that cause WSBF damage are due to the activated Maillard reaction and the lipid peroxidation reaction induced by oxidative stress. In order to suppress the occurrence of this disorder, it is important to harvest the fruit before the reducing sugar concentration increases due to the activation of neutral invertase in the latter half of the maturation period. In WSBF-susceptible cultivars, the occurrence of the disorder can be suppressed by reducing the amount of thinning and suppressing fruit growth (Sakuma et al. 1995).

In addition, defoliation treatment and/or shading treatment during fruit ripening may also be an effective control method if the occurrence of damage is predicted in advance (Sakuma et al. 1998).

Supplementary Information The online version contains supplementary material available at https://doi.org/10.1007/s10725-021-00765-x.

Acknowledgements NF is grateful for the assistance with the fieldwork by A. Sugiyama, H. Tsugawa, and T. Yamamura of Ishikawa Prefectural University.

Author contributions NF and RW conceived and designed the research. NF wrote the manuscript. NF and RW performed immunohistochemical observation and contributed to data analysis. RW and TH contributed the gene expression analysis. All authors approved the final version of the manuscript.

Data availability The data will be made available on reasonable request.

References

Ahmed MU, Brinkmann FE, Degenhardt TP, Thorpe SR, Baynes JW (1997) N-epsilon-(carboxyethyl)lysine, a product of the chemical modification of proteins by methylglyoxal, increases with AGE in human lens proteins. Biochem J 324:565–570. https://doi.org/10.1042/bj3240565

Akuta T, Zaki MH, Yoshitake J, Okamoto T, Akaike T (2006) Nitrative stress through formation of 8-nitroguanosine: insights into microbial pathogenesis. Nitric Oxide 14:101–108. https://doi.org/10.1016/j.niox.2005.10.004

Al-Abed Y, Bucala R (1995) Nε-carboxymethyllysine formation by direct addition of glyoxal to lysine during the maillard reaction. Bioorg Med Chem Lett 5:2161–2162

Ames JM (1992) The maillard reaction. Biochem food proteins. BJF Hudson, Springer Boston, pp. 99–153. https://doi.org/10.1016/0960-894X(95)00375-4

Anderson MM, Heinecke JW (2003) Production of N-(Carboxymethyl) lysine is impaired in mice deficient in NADPH oxidase. A role for phagocyte-derived oxidants in the formation of advanced glycation end products during inflammation. Diabetes 52:2137–2143. https://doi.org/10.2337/diabetes.52.8.2137

Bianco RL, Rieger M (2002) Partitioning of sorbitol and sucrose catabolism within peach fruit. J Amer Soc Hort Sci 127:115–121. https://doi.org/10.21273/JASHS.127.1.115

DiMarco T, Giulivi C (2007) Current analytical methods for the detection of dityrosine, a biomarker of oxidative stress, in biological samples. Mass Spectrom Rev 26:108–120. https://doi.org/10.1002/mas.20109

Fukuoka N, Hamada T (2021) Effects of heat stress on the biological maillard reaction, oxidative stress, and occurrence of internal browning in Japanese radish (*Raphanus sativus* L.). J Plant Physiol 256:1–10. https://doi.org/10.1016/j.jplph.2020.153326

Fukuoka N, Miyata M, Hamada T, Takeshita E (2018) Histochemical observations and gene expression changes related to internal browning in tuberous roots of sweet potato (*Ipomea batatas*). Plant Sci 274:476–484. https://doi.org/10.1016/j.plantsci.2018.07.004

Fukuoka N, Hirabayashi H, Hamada T (2020) Oxidative stress via the maillard reaction is associated with the occurrence of internal browning in roots of sweetpotato (*Ipomoea batatas*). Plant Physiol Biochem 154:21–29. https://doi.org/10.1016/j.plaphy.2020.05.009

Glomb MA, Lang G (2001) Isolation and characterization of glyoxal-arginine modifications. J Agric Food Chem 49:1493–1501. https://doi.org/10.1021/jf001082d

Hashizume H, Tanase K, Shiratake K, Mori H, Yamaki S (2003) Purification and characterization of two soluble acid invertase isozymes from Japanese pear fruit. Phytochem 63:125–129. https://doi.org/10.1016/S0031-9422(03)00107-9

Ishikawa Fruit Tree Gardening Association (1987) Ishikawa Fruit Tree. 1–54.

Itai A, Hatanaka R, Irie H, Murayama H (2015) Effects of storage temperature on fruit quality and expression of sucrose phosphate synthase and acid invertase genes in Japanese pear. Hort Sci 84:227–232. https://doi.org/10.2503/hortj.MI-047

Jambunathan N (2010) Determination and detection of reactive oxygen species (ROS), lipid peroxidation, and electrolyte leakage in plants. Plant Stress Toler 639:291–297. https://doi.org/10.1007/978-1-60761-702-0_18

Kajiura I, Yamaki S, Omura M, Shimura I (1976) Watercore in japanese pear (*Pyrus serotina* Rehder var. 'Culta' Rehder). I. Description of the disorder and its relation to fruit maturity. Sci Hortic 4:261–270. https://doi.org/10.1016/0304-4238(76)90049-2

Kim SH, Hamada T (2005) Rapid and reliable method of extracting DNA and RNA from sweetpotato, *Ipomoea batatas* (L.). Lam Biotechnol Lett 27:1841–1845. https://doi.org/10.1007/s10529-005-3891-2

Lepetsos P, Papavassiliou AG (2016) ROS/oxidative stress signaling in osteoarthritis. Biochim Biophys Acta Mol Basis Dis 1862:576–591. https://doi.org/10.1016/j.bbadis.2016.01.003

Manuel A, Matamoros MA, Kim A, Peñuelas M, Ihling C, Griesser E, Hoffmann R, Fedorova M, Frolov A, Becana M (2018) Protein carbonylation and glycation in Legume Nodules. Plant Physiol 177:1510–1528. https://doi.org/10.1104/pp.18.00533

Matsumoto Y, Sumiya E, Sugita T, Sekimizu K (2011) An invertebrate hyperglycemic model for the identification of anti-diabetic drugs. PLoS ONE 6:1–11. https://doi.org/10.1371/journal.pone.0018292

Murata M (2019) Maillard reaction and browning: chemistry of browning reaction between saccharides and amino acids. Kagaku Seibutsu 57:213–220. https://doi.org/10.1271/kagakutoseibutsu.57.213

Murata M, Homma S (1998) Recent progress in polyphenol oxidase and control of enzymatic browning. Nippon Shokuhin Kagaku Kogaku Kaishi 45:177–185. https://doi.org/10.3136/nskkk.45.177

Nishikawa T, Edelstein D, Du XL, Yamagishi S, Matsumura T, Kaneda Y, Yorek MA, Beebe D, Oates PJ, Hammes HP, Giardino I, Brownlee M (2000) Normalizing mitochondrial superoxide production blocks three pathways of hyperglycaemic damage. Nature 404:787–790. https://doi.org/10.1038/35008121

Nishitani C, Inoue E, Saito T, Ogata N, Kita K, Gonai T, Kasumi M, Ishii R, Sawamura Y, Takada N, Nakamura Y, Kobayashi M, Yano K, Terakami S, Yamamoto T (2020) Transcriptome analysis of watercore in *Pyrus pyrifolia* by comparing pairs of susceptible and resistant F1 sibs. Sci Hortic 264:1–9. https://doi.org/10.1016/j.scienta.2019.109136

Paudel G, Bilova T, Schmidt R, Greifenhagen U, Berger R, Tarakhovskaya E, Stöckhardt S, Balcke GU, Humbeck K, Brandt W, Sinz A, Vogt T, Birkemeyer C, Wessjohann L, Frolov A (2016) Osmotic stress is accompanied by protein glycation in *Arabidopsis thaliana*. J Exp Bot 67:6283–6245. https://doi.org/10.1093/jxb/erw395

Portero-Otin M, Nagaraj RH, Monnier VM (1995) Chromatographic evidence for pyrraline formation during protein glycation in vitro and in vivo. Biochim Biophys Acta 1247:74–80. https://doi.org/10.1016/0167-4838(94)00209-y

Sakuma F, Katagiri S, Orimoto Y, Tahira K, Umeya T, Suzuki Y, Hiyama H, Ishizuka Y (1995) Factors which induce watercore in Japanese pear (*Pyrus Pyrifolia* Nakai. Cv. Housui). Effect of tree vigor on the occurrence of watercore. Bull Hort Inst Ibaraki Agric Cent 3:1–10. 2010571139.pdf (affrc.go.jp)

Sakuma F, Katagiri S, Tahira K, Umeya T, Hiyama H (1998) Effects of defoliation and fruit thinning on occurrence of watercore in Japanese pear (*Pyrus Pyrifolia* Nakai) 'Housui.' J Japan Soc Hort Sci 67:381–385. https://doi.org/10.2503/jjshs.67.381

Singh R, Barden A, Mori T, Beilin L (2001) Advanced glycation end-products: a review. Diabetologia 44:129–146. https://doi.org/10.1007/s001250051591

Tanase K, Yamaki S (2000) Sucrose synthase isozymes related to sucrose accumulation during fruit development of Japanese pear (*Pyrus pyrifolia* Nakai). J Japan Soc Hort Sci 69:671–676. https://doi.org/10.2503/jjshs.69.671

Teo G, Suzuki Y, Uratsu SL, Lampinen B, Ormonde N, Hu WK, DeJong TM, Dandekar AM (2006) Silencing leaf sorbitol synthesis alters long-distance partitioning and apple fruit quality. Proc Natl Acad Sci USA 103:18842–18847. https://doi.org/10.1073/pnas.0605873103

Teshima Y, Takahashi N, Nishio S, Saito S, Kondo H, Fukui A, Aoki K, Yufu K, Nakagawa M, Saikawa T (2014) Production of reactive oxygen species in the diabetic heart; Roles of mitochondria and NADPH oxidase. Circulation J 78:300–304. https://doi.org/10.1253/circj.cj-13-1187

Trafdar A, Pula G (2018) The roke of NADPH oxidases and oxidative stress in neurodegenerative disorders. Int J Mol Sci 19:3824. https://doi.org/10.3390/ijms19123824

Uchida K (1999) Current status of acrolein as a lipid peroxidation product. Trends Cardiovasc Med 9:109–113. https://doi.org/10.1016/s1050-1738(99)00016-x

Wang D, Ma Q, Belwal T, Li D, Li W, Ki L, Luo Z (2020) High carbon dioxide treatment modulates sugar metabolism and maintains the quality of fresh-cut pear fruit. Molecules 25:4261. https://doi.org/10.3390/molecules25184261

Wells-Knecht KJ, Brinkmann E, Baynes JW (1995) Characterization of an imidazolium salt formed from glyoxal and N.alpha.-hippuryllysine; A model for maillard reaction crosslinks in proteins. J Org Chem 60:6246–6247. https://doi.org/10.1021/jo00125a001

Yamaki S (2007) Fruit sinking ability and hypertrophy mechanism. Horticultural physiology. S Yamaki, Buneido Tokyo Japan pp. 161–169.

Yamaki S, Moriguchi T (1989) Seasonal fluctuation of sorbitol-related enzymes and invertase activities accompanying maturation of Japanese pear (*Pyrus serotina* Rehder var. *culta* Rehder) fruit. J Japan Soc Hort Sci 57:602–607. https://doi.org/10.2503/jjshs.57.602

Yamaki S, Kajiura I, Omura M, Matsuda K (1976) Watercore in Japanese pear (*Pyrus serotina* Rehder var. 'Culta' Rehder). II. Chemical changes in watercored tissue. Sci Hort 4:271–277. https://doi.org/10.1016/0304-4238(76)90050-9

Zhang H-p, Wu J-y, Tao S-t, Wu T, Qi K-j, Zhang S-j, Wang J-z, Huang W-j, Wu J, Zhang S-l (2014) Evidence for apoplasmic phloem unloading in pear fruit. Plant Mol Biol Rep 32:931–939. https://doi.org/10.1007/s11105-013-0696-7